Lake-Effect Rains over Lake Victoria and Their Association with Mesoscale Convective Systems

SHARON E. NICHOLSON,[a] DOUGLAS KLOTTER,[a] AND ADAM T. HARTMAN[a]

[a] *Department of Earth, Ocean, and Atmospheric Science, Florida State University, Tallahassee, Florida*

(Manuscript received 16 October 2020, in final form 16 March 2021)

ABSTRACT: This article examined rainfall enhancement over Lake Victoria. Estimates of overlake rainfall were compared with rainfall in the surrounding lake catchment. Four satellite products were initially tested against estimates based on gauges or water balance models. These included TRMM 3B43, IMERG V06 Final Run (IMERG-F), CHIRPS2, and PERSIANN-CDR. There was agreement among the satellite products for catchment rainfall but a large disparity among them for overlake rainfall. IMERG-F was clearly an outlier, exceeding the estimate from TRMM 3B43 by 36%. The overestimation by IMERG-F was likely related to passive microwave assessments of strong convection, such as prevails over Lake Victoria. Overall, TRMM 3B43 showed the best agreement with the ''ground truth'' and was used in further analyses. Overlake rainfall was found to be enhanced compared to catchment rainfall in all months. During the March–May long rains the enhancement varied between 40% and 50%. During the October–December short rains the enhancement varied between 33% and 44%. Even during the two dry seasons the enhancement was at least 20% and over 50% in some months. While the magnitude of enhancement varied from month to month, the seasonal cycle was essentially the same for overlake and catchment rainfall, suggesting that the dominant influence on overlake rainfall is the large-scale environment. The association with mesoscale convective systems (MCSs) was also evaluated. The similarity of the spatial patterns of rainfall and MCS count each month suggested that these produced a major share of rainfall over the lake. Similarity in interannual variability further supported this conclusion.

SIGNIFICANCE STATEMENT: The article underscores the difficulty of IMERG-F and other passive microwave retrievals in assessing rainfall over inland water bodies.

KEYWORDS: Africa; Inland seas/lakes; Lake effects; Mesoscale systems

1. Introduction to the problem

The inland lakes of the Rift Valley are one of East Africa's greatest resources (Fig. 1). They provide water for herds, agriculture, and hydroelectric power. They sustain the fishing industry and serve as attractions for the regions' important tourist industry. Lake Victoria alone provides the livelihood for over 30 million people. In recent years, droughts, increasing temperatures, and increased water consumption have led to dramatically decreased levels of lakes such as Turkana and Victoria. This has created considerable hardship in the population around the lakes. In view of the changes already occurring and the sensitivity of the region to climatic change, the longer-term response of the lakes to global warming is a serious concern (Akurut et al. 2014; Di Baldassarre et al. 2011).

Reliable estimates of lake water balance are critical in evaluating this response and in projecting future water resources. Such estimates are important in interpreting the vast paleoclimatic records obtained from the lakes. They are also required to translate the now routinely disseminated seasonal rainfall forecasts into surface water availability (Ogallo et al. 2008). Assessing water balance for the East African lakes is a complex task, hindered by the difficulty in obtaining meteorological and hydrological data. Estimates have been published for several of the East African lakes. Most estimates are for Lake Victoria (Swenson and Wahr 2009; Vanderkelen et al. 2018; Kizza et al. 2012; Tate et al. 2004; Yin and Nicholson 1998) and Lake Tana (Tigabu et al. 2019; Rientjes et al. 2011; Wale et al.2009; Chebud and Melesse 2009; Kebede et al. 2006). Estimates have also been made for Lake Tanganyika (Bergonzini et al. 2002), Lake Turkana (Velpuri et al. 2012), Lake Malawi (Lyons et al. 2011), Lake Kivu (Bergonzini 1998; Muvundja et al. 2014), Lake Rukwa (Bergonzini 1998), and Lake Edward (Lehman 2002).

In all cases except Lake Turkana, rainfall over the lake provides the greatest input into the lake's water balance. However, few have included estimates of rainfall directly over the lake. This is critical because over several of the lakes the combined effects of mountain/valley winds and land/lake breezes enhance rainfall over the lake (Anyah et al. 2006; Thiery et al. 2015). Establishing that component of the water balance is a major challenge (Kizza et al. 2012).

The varied estimates for Lake Victoria illustrate the problem. Some of the earlier published values of overlake rainfall range between 1145 and 1850 mm yr^{-1} (Yin and Nicholson 1998). Ba and Nicholson (1998), applying an algorithm to Meteosat data, found an enhancement of 27%. Kizza et al. (2012) found that estimates from Tropical Rainfall Measuring Mission (TRMM) 3B43 and Precipitation Estimation from Remotely Sensed Information Using Artificial Neural Networks–Climate Data Record (PERSIANN-CDR) differed substantially.

Corresponding author: Sharon E. Nicholson, snicholson@fsu.edu

DOI: 10.1175/JHM-D-20-0244.1

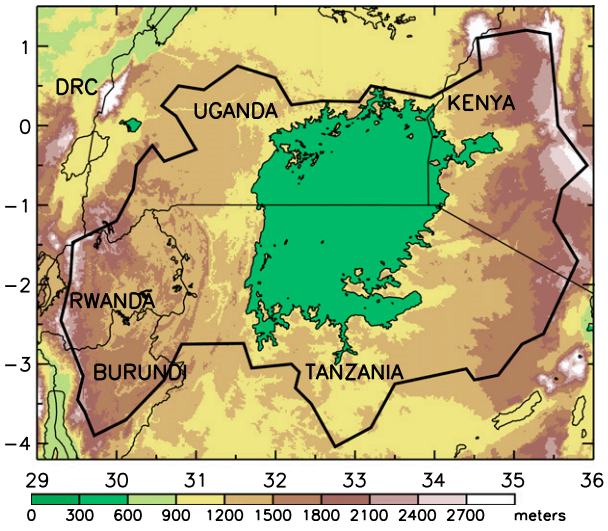

FIG. 1. Lake Victoria and surrounding topography. The solid black line shows the lake catchment.

The enhancement of rainfall over the lake, compared with the surrounding catchment, was assessed by TRMM 3B43 as 28% but by PERSIANN-CDR as 85%. The modeling study of Thiery et al. (2015) suggested the enhancement was as high as 82%.

Lake Victoria also illustrates why accurate assessment of overlake rainfall is of utmost importance. Overlake rainfall represents over 80% of its input (Yin and Nicholson 1998) and in some years it is nearly twice as great as rainfall over the surrounding basin. Thus, overlake rainfall is a critical determinant of lake level, which in turn plays a major role in determining the flow of the White Nile, the life-blood of Sudan, South Sudan, and Egypt. Sene (2000) calculated that a 1-m rise of Lake Victoria can increase flow throughout the White Nile system by 70%–80%. Such a rise occurred in 1961, a year in which overlake rainfall reached roughly 2500 mm (Yin and Nicholson 2002).

The overall goal of this study is to produce an accurate assessment of rainfall enhancement over Lake Victoria on a seasonal basis. This will necessarily be based on satellite assessments of rainfall, so that a secondary goal is to determine which satellite product or products provide the most reliable estimates of overlake rainfall. It goes beyond prior work on the subject by deriving the seasonal cycle of the enhancement, examining the relationship between rainfall and mesoscale convective systems (MCSs), and contrasting conditions over the lake during the two rainy seasons.

In this article the data utilized are described in section 2. Intercomparison of the satellite products and a comparison of those products with gauge data are presented in section 3. Section 4 considers the seasonal cycle of lake-effect rains and the association with MCSs. Section 5 discusses possible reasons for the positive bias of the Integrated Multisatellite Retrievals for Global Precipitation Measurement (GPM) V06 Final Product (IMERG-F) in estimating overlake rainfall. A summary and conclusions are present in section 6.

2. Data and methodology

a. Choice of satellite products

A large number of satellite rainfall products are available for the equatorial Africa (Nicholson et al. 2019). Unfortunately, few have been examined over Lake Victoria or near the lake. Tan et al. (2019) showed that IMERG-F could realistically reproduce the diurnal cycle over Lake Victoria and Haile et al. (2013) showed the same for TRMM 3B42 and Climate Prediction Center morphing technique (CMORPH) CRT. However, all three products appeared to overestimate rain rate. Kizza et al. (2012) considered the Lake Victoria catchment and concluded that TRMM 3B43 outperformed PERSIANN CDR. Dezfuli et al. (2017) compared the IMERG-V04A product with TRMM 3B42 V7 and the Climate Hazards Group Infrared Precipitation with Station Data (CHIRPS) dataset in an area near Kisumu, Kenya, on the shore of Lake Victoria. They noted that TRMM showed better agreement with gauge data for the annual cycle and that IMERG showed better agreement for the diurnal cycle. Both appeared to outperform CHIRPS.

Satellite validation for regions in or near the Congo basin, which lies just to the west of Lake Victoria, have also demonstrated that TRMM products, PERSIANN-CDR, and CHIRPS2 tend to perform best in that region (Beighley et al. 2011; Munzimi et al. 2015; Camberlin et al. 2019) In a study at the monthly scale for the Congo basin and adjacent regions, Nicholson et al. (2019) evaluated nine satellite rainfall products and found that CHIRPS2, PERSIANN-CDR, and TRMM 3B43 showed the best agreement with gauge data. The performance of those products was particularly strong for an eastern sector that included part of the Lake Victoria catchment. Awange et al. (2016) and Dinku et al. (2018) further showed that both TRMM 3B42 and PERSIANN-CDR compare well with gauge data in equatorial eastern Africa and outperformed other available products. None of the aforementioned studies examined IMERG.

In view of the disparity in the assessments of the various satellite rainfall retrievals and the limited examination of IMERG, the choice of the best product for this study was not immediately clear. The monthly products that were consistently found to perform well in equatorial Africa were CHIRPS2, PERSIANN-CDR, and TRMM 3B43. To determine the best product or products for this study, these three products plus IMERG-F are evaluated and compared with gauge data and other estimates of overlake rainfall in section 3. The details about these products are given below in section 2b.

b. Satellite rainfall products examined in this study

The Tropical Rainfall Measuring Mission (TRMM) satellite was a joint mission between NASA and the Japanese Aerospace Exploration Agency. It was specifically designed to measure tropical rainfall globally. The product used here, 3B43 V7, is a monthly accumulation of the 3B42 V7 product that merges precipitation estimates from several passive microwave (PMW) sensors with microwave-calibrated infrared-based precipitation estimates and then performs bias adjustment using monthly

accumulated rain gauge analysis from GPCC (Huffman et al. 2007, 2015; Huffman and Bolvin 2014). TRMM 3B43 has a spatial resolution of 0.25°. Data are available for 1998–2019.

IMERG V06B combines PMW satellite retrievals from whatever constellation of satellites is operating in Earth orbit, at a given time and location, to estimate precipitation over the majority of Earth's surface (Huffman et al. 2019). Precipitation estimates are derived from a fully parametric retrieval algorithm based on PMW brightness temperature (GPROF). The PMW estimates are also merged with infrared (IR) estimates and eventually calibrated and merged with gauge data. The current algorithm fuses the early precipitation estimates collected in 2000–14 from the TRMM satellite with more recent estimates collected from the GPM *Core Observatory* satellite, launched in 2014. These serve as both input and calibrators. However, the bulk of the input data are from the constellation of other PMW sensors, with geo-infrared fill-in. IMERG V06B has 0.1° and half-hour resolution. Here we used the Final Run (IMERG-F), which has gauge-adjusted estimates. Data are available for 2001–20.

CHIRPS2 (Funk et al. 2015) is based on thermal IR brightness temperature from geostationary satellites. It has a spatial resolution of 0.05° and a daily temporal resolution. CHIRPS2 begins in 1981 and extends through 2020. It is a result of a collaboration between the University of California, Santa Barbara, and USGS. CHIRPS2 is based on cold-cloud duration from two geosynchronous thermal IR archives produced by NOAA. One is the 1981–2008 Globally Gridded Satellite (GridSat) produced by the National Climate Data Center. The second is the 2000–present NOAA Climate Prediction Center dataset (CPC 4-km merged IR). The thermal IR data are merged with African gauge data, using ''smart'' interpolation techniques that take the spatial correlation structure into account. The CHIRPS2 data have low bias and better gauge coverage over Africa compared to other similar products (Dezfuli et al. 2017).

PERSIANN-CDR (Ashouri et al. 2015) is also based on geostationary thermal IR brightness temperature, with a neural network approach applied to produce the precipitation estimates. The product is calibrated using NCEP/NCAR precipitation forecasts. It is bias corrected with GPCP precipitation estimates on a monthly basis, such that PERSIANN-CDR and GPCP monthly totals are consistent. Its spatial resolution is 0.25°. Data are available for 1983–2020.

c. Other data

Rainfall gauge data are obtained from two sources, the NIC131 gauge dataset of the first author (Nicholson et al. 2018) and the Centennial Trends (CenTrends) gridded dataset (Funk et al. 2015). These are not totally independent datasets, as most of the NIC131 stations have been incorporated into CenTrends. However, the latter includes many stations not in NIC131 and statistical methods have been applied to producing a complete grid of rainfall data for eastern Africa. In the current region of study, however, more stations are available in NIC131, especially for Rwanda and Burundi. Also, NIC131 includes data through 2018 while CenTrends extends only through 2014.

Counts and locations of MCSs are taken from a dataset of Hartman (2016, 2020). The MCS tracking utilized the GridSat-B1 dataset of NOAA's National Center for Environmental Information. That dataset is 3-hourly and on a 0.07° equal-angle grid. Environmental parameters associated with the MCSs were derived from NASA's Modern-Era Retrospective Analysis for Research Applications, Version 2 (MERRA2), which has a resolution of 0.5° latitude and 0.625° longitude. The MCS dataset has a 0.5° and 3-h resolution, covers the 6 months of March–May and September–November, and runs from 1983 to 2015.

3. Evaluation of satellite rainfall products

The goal of this analysis is to determine which of the four satellite products provides the most realistic representation of rainfall in the Lake Victoria region, with special emphasis on overlake rainfall. A complete validation of the products is not intended. The four satellite products are compared based on annual means and on means for April, the wettest month over most of the region. Calculations are based on the years common to all four, 2001–18. The year 2019 is excluded because few gauge records cover that year.

a. Intercomparison of satellite products

Figure 2a shows mean annual rainfall over Lake Victoria and surrounding regions from the four monthly satellite products and averaged for the years 2001–18. There is clearly a large spread among the four products with respect to overlake rainfall. CHIRPS2 and PERSIANN-CDR suggest values of 1200–2000 mm over most of the lake. TRMM 3B43 and IMERG-F show much larger values, with the latter showing rainfall in excess of 3000 mm over about half of the lake. There is much better agreement for rainfall over the catchment, with the exception of PERSIANN-CDR showing very high rainfall to the northeast of the lake. All four products show rainfall on the order of 800–1400 mm over most of the catchment. Three of the four show 1400–2000 mm just to the north and east of the lake, while PERSIANN-CDR suggests values in excess of 3000 mm.

Figure 3a shows mean rainfall for April, the month in which the lake-effect rains are best developed. As with annual rainfall, the rainfall values over the catchment are fairly similar for the four products. Exceptions are the strong maximum northeast of the lake in PERSIANN-CDR (as also seen in annual data) and the comparatively low values to the west and south of the lake in PERSIANN-CDR (large areas with rainfall below 100 mm). In contrast, there are pronounced differences in the estimates of overlake rainfall. IMERG-F shows April rainfall exceeding 320 mm over nearly the entire lake and large areas with rainfall exceeding 480 mm. TRMM 3B43 and CHIRPS2 show only small sectors with rainfall reaching 320 mm. Both show rainfall on the order of 240–360 mm over roughly half of the lake. The estimates of PERSIANN-CDR are considerably lower, with a mean of roughly 160–280 mm over nearly the entire lake.

b. Comparison of satellite products with gauge data over the catchment

Typically, gauge data are used as ''ground truth'' for satellite rainfall estimates. Unfortunately, in the region of interest the

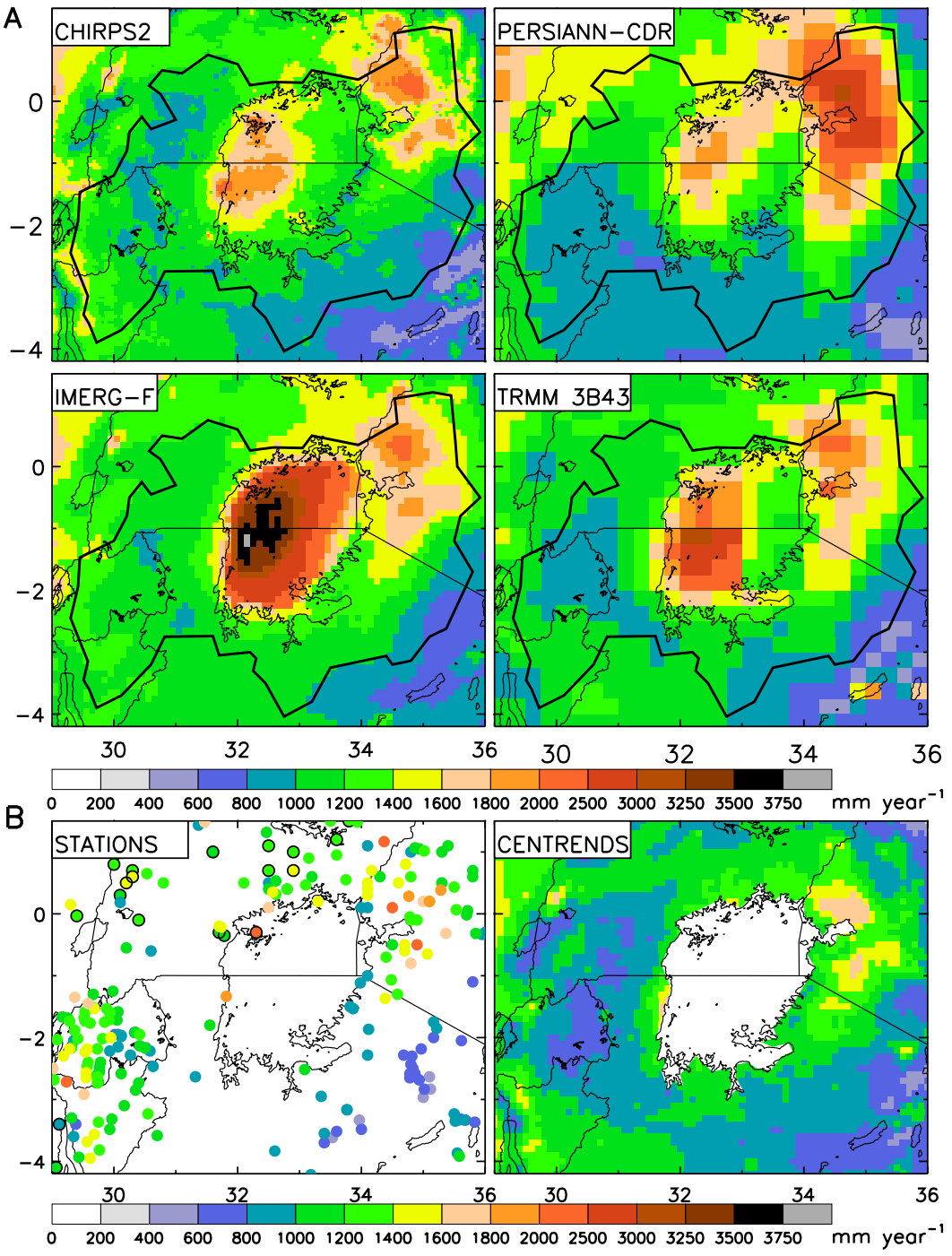

FIG. 2. (a) Annual rainfall (mm) from four satellite products, averaged for the years 2001–18. (b) Mean annual rainfall (mm) from NIC131 (2001–18) and CenTrends (2001–14).

gauge datasets are less than adequate because of the difficulty in obtaining recent gauge records. Consequently, the station network changes over time and at certain locations and times coverage is sparse. However, the gauge products used here, NIC131 and CenTrends, include more stations in this region of Africa than any other available gauge dataset (Funk et al. 2015). Yet, there are still numerous gaps. Within the period 2001–18 both NIC131 and CenTrends include a large number of stations in Kenya and Tanzania. NIC131 includes extensive records in Burundi and Rwanda but CenTrends does not (Funk et al. 2015). Neither include extensive up-to-date records over Uganda. However, NIC131 includes extensive long-term

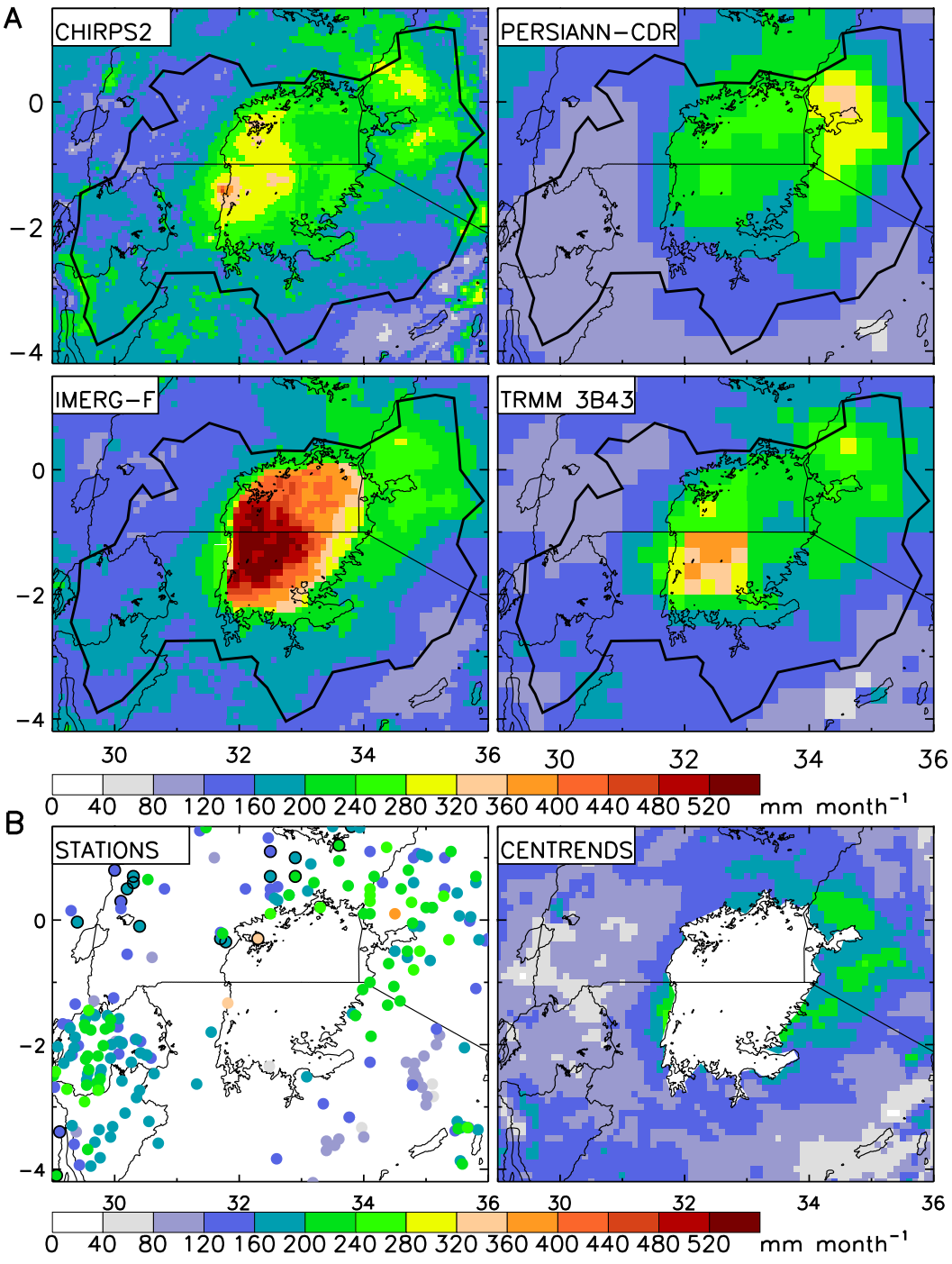

FIG. 3. (a) April rainfall (mm) from four satellite products, averaged for the years 2001–18. (b) Mean April rainfall (mm) from NIC131 (2001–18) and CenTrends (2001–14).

records for Uganda. Note that CenTrends provides continual spatial and temporal coverage throughout the period 2001–18. However, the errors in the estimates are large where gauge records are sparse (Funk et al. 2015).

The approach taken here is to produce maps of April and annual rainfall from both gauge datasets and compare them with satellite estimates of rainfall. Hardly ideal, this provides at least some rudimentary ground truth by which to assess the best satellite product to use here. Given the differences in spatial and temporal coverage and spatial resolution, excellent agreement in magnitude cannot be expected but the spatial patterns provided by the gauges are reliable and provide a

useful comparison with the satellite records. This provides some guidance in determining which satellite product to use in further analyses.

Figure 2b shows the annual mean based on 286 gauge records from NIC131 and on the CenTrends dataset. The NIC131 records have been averaged for each 0.5° grid box. All grid boxes with one or more stations are indicated. When adequate data are available, averages are for the period 2001–18, as with the satellite averages. Most stations in the Democratic Republic of the Congo and Uganda do not cover that period. To maximize spatial coverage, the long-term mean is plotted for additional stations. These are indicated by dots enclosed in a thick black line. The long-term mean has been fairly stable in this region, so that a comparison of the long-term mean with the 2001–18 mean is reasonable. For CenTrends, the means are for the period 2001–14, thus covering most of the years averaged for the satellite estimates. A comparison for the 2001–14 period was also made, and the results are similar.

The comparison suggests that all four satellite products provide reasonable estimates of rainfall over the catchment (see Fig. 1 for location). The satellite estimates and the gauges show that over most of the catchment mean annual rainfall is on the order of 800–1200 mm. An area of higher rainfall lies to the north and east of the lake. In all cases, rainfall peaks just to the northeast, with gauges and three of the satellite estimates indicating 1400–2500 mm. The PERSIANN-CDR estimate of 1800 mm to over 3000 mm is an unrealistic outlier. Overall, CHIPRS2 and TRMM 3B43 appear to show the best agreement with gauge data in terms of spatial distribution and magnitude.

Figure 3b shows the April mean from NIC131 gauge data and from CenTrends. Given the contrast in spatial resolution and temporal coverage of the two datasets, only general agreement can be expected. Along the western lake shore, including the western islands, and to the north, east and south of the lake, there is good agreement between NIC131 and CenTrends. However, in southeastern Uganda NIC131 shows somewhat higher values. NIC131 shows two rainfall maxima in the west, one over the Ssese Islands in the northwest and another at ~1.5°S. CenTrends shows some semblance of the latter. NIC131 again shows somewhat higher values, 320–360 mm, compared to 280–320 mm in CenTrends. Both show rainfall on the order of 160–200 mm directly along the shore to the north and west. To the northeast of the lake both show rainfall on the order of 160–240 mm. The lower values further south and southeast are also in general agreement, although much of that area is outside the lake's catchment. The major area of disagreement is in the mountainous terrain to the west of the lake, over Rwanda and Burundi. CenTrends shows values on the order of 80–160 mm, while NIC131 shows values on the order of 120–200 mm. Given the near absence of gauges in CenTrends in this area and the large number of NIC131 stations, the latter is considered more realistic.

Three of the four satellite products indicate values in agreement with the gauges in the maximum to the northeast, i.e., rainfall on the order of 200–280 mm for the most part. As with annual data, PERSIANN greatly overestimates this maximum. Both CHIRPS2 and IMERG-F are in agreement with the gauges to the southwest of the lake, i.e., rainfall on the order of 160–220 mm. All four products show the minimum southeast of the lake, where rainfall is generally between 80 and 120 mm.

As stated earlier, the goal of this analysis is not a validation of the satellite products. Its purpose is to decide which of the four products considered shows the best agreement with gauges. Based on the comparison with gauge data, TRMM 3B43, IMERG-F, and CHIRPS2 would all provide reasonable estimates of catchment rainfall. PERSIANN-CDR appears to provide the largest discrepancy with respect to gauge data. It is an outlier in particular over the highlands in the eastern portion of the lake's catchment. However, the final decision as to what product to use in the remaining analyses depends on their estimates of overlake rainfall.

c. Comparison of satellite estimates of overlake rainfall

Validating estimates of overlake rainfall is more difficult because there are few direct measurements of rainfall over the lake. However, a handful of measurements are available from islands in the lake, such as the Ssese Islands near Entebbe in the northwest and Nabuyongo Island toward the center of the lake (Flohn and Fraedrich 1966). Relevant information is also available from convective and hydrological modeling studies (e.g., Fraedrich 1972; Yin and Nicholson 1998) and global radiation over the lake (Datta 1981). These allow for comparison with the long-term means of overlake rainfall and rainfall maxima and with the spatial pattern of rainfall over the lake, all of which are relevant hydrological characteristics.

Fraedrich (1968, 1971) evaluated radiosonde measurements over the lake and utilized them in producing a convective model for circulation over Lake Victoria (Fraedrich 1972). Based on that model, nine island rainfall stations, and a few shoreline stations, Flohn and Burkhardt (1985) produced the map of overlake rainfall shown in Fig. 4. Datta (1981) produced a map of April rainfall based on shoreline and island stations. It shows three separate maxima. One is over the Ssese Islands in the northwest south of Entebbe, another stretches from Nabuyongo Island westward to the coast, and a third is over a group of islands in the southeast north of Mwanza.

In terms of the spatial pattern of overlake rainfall, that of IMERG-F qualitatively resembles that in Fig. 4. However, IMERG-F (Fig. 2a) shows 3000–4000 mm over nearly half of the lake, which is arguably too high. The spatial patterns of rainfall from TRMM 3B43 and CHIRPS2 are also consistent with Fig. 4, with rainfall in the east being clearly lower than in the west. Notably, a map of global radiation from Datta (1981) (not shown) indicates a minimum that corresponds closely with the area in TRMM 3B43 and CHIRPS2 where rainfall exceeds 1600 mm yr^{-1} and the area in IMERG-F where rainfall exceeds 3000 mm yr^{-1}. CHIRPS2 is the only product that shows maxima in the three locations indicated in the Datta map.

In terms of the magnitude of the maximum over the lake, Fig. 4 shows roughly 3000 mm over Nabuyongo Island. This is consistent with the estimates from TRMM 3B43, which gives a maximum of 3040 mm (Fig. 2a) and IMERG-F, which shows a maximum of roughly 3250 mm at the location of Nabuyongo.

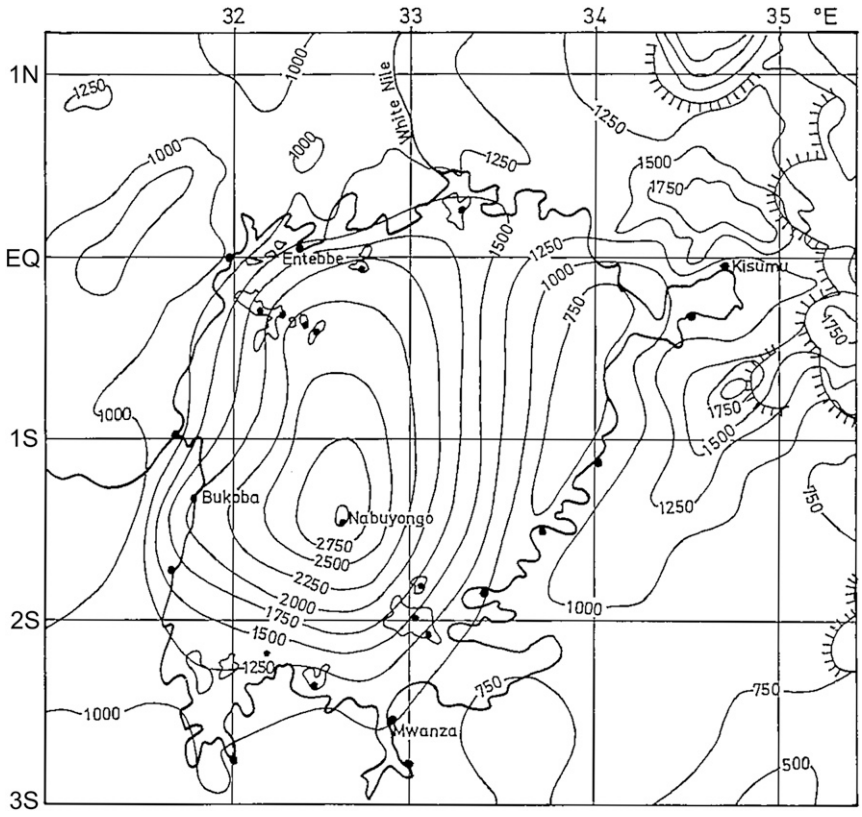

FIG. 4. Map of annual rainfall in mm over Lake Victoria and the surrounding region (based on Flohn and Burkhardt 1985).

CHIRPS2 and PERSIANN-CDR, with maxima on the order of 1800–2000 mm, clearly underestimate overlake rainfall.

Estimates of long-term means for overlake rainfall appeared in several studies. Flohn (1983) gave a value of 1690 mm for the period 1945–84, but his later work (Flohn and Burkhardt 1985) estimated the mean to be between 1630 and 1660 mm during the period 1950–79. Howell et al. (1988) produced an estimate of 1810 mm for the period 1956–78, extrapolating overlake rainfall from gauge data near the lake. Yin and Nicholson (1998) estimated overlake rainfall from catchment rainfall, using a relationship between the two that was derived by Ba and Nicholson (1998) from Meteosat infrared data. Their estimate, also for the period 1956–78, was 1791 mm. Using a somewhat different methodology, Nicholson and Yin (2002) estimated overlake rainfall for the period 1931–94 to be 1668 mm. Based on water balance considerations, the error in calculated overlake rainfall was estimated as roughly 6%. This suggests that the calculated values of Nicholson and Yin (2002) are very realistic.

In comparison, overlake rainfall estimated from TRMM 3B43 for the period 2001–18 is 1717 mm (Table 1), reasonably close to the estimates of Nicholson and Yin (2002) and Yin and Nicholson (1998). The estimates from CHIRPS2 and PERSIANN-CDR are much lower, 1411 and 1510 mm, respectively, while IMERG-F gives a value of 2338 mm. The estimates of rainfall over the catchment (see Fig. 2) are considerably less diverse, ranging from 1136 mm for CHIRPS2 to 1248 mm for IMERG-F (Table 1). The large disparity in overlake

TABLE 1. Mean annual overlake and catchment rainfall (mm) over three East African lakes, as estimated by four satellite products. Rainfall is averaged for the years 2001–18.

Location	Area (km^2)	TRMM 3B43	IMERG-F	CHIRPS2	PERSIANN-CDR
Victoria Lake	68 800	1688	2338	1424	1477
Tanganyika Lake	32 000	1300	1599	1119	1199
Malawi Lake	29 600	1511	1632	1284	1310
Victoria Catchment	184 000	1185	1248	1161	1150
Tanganyika Catchment	263 000	1079	1115	1084	957
Malawi Catchment	6593	1117	1158	1102	1168

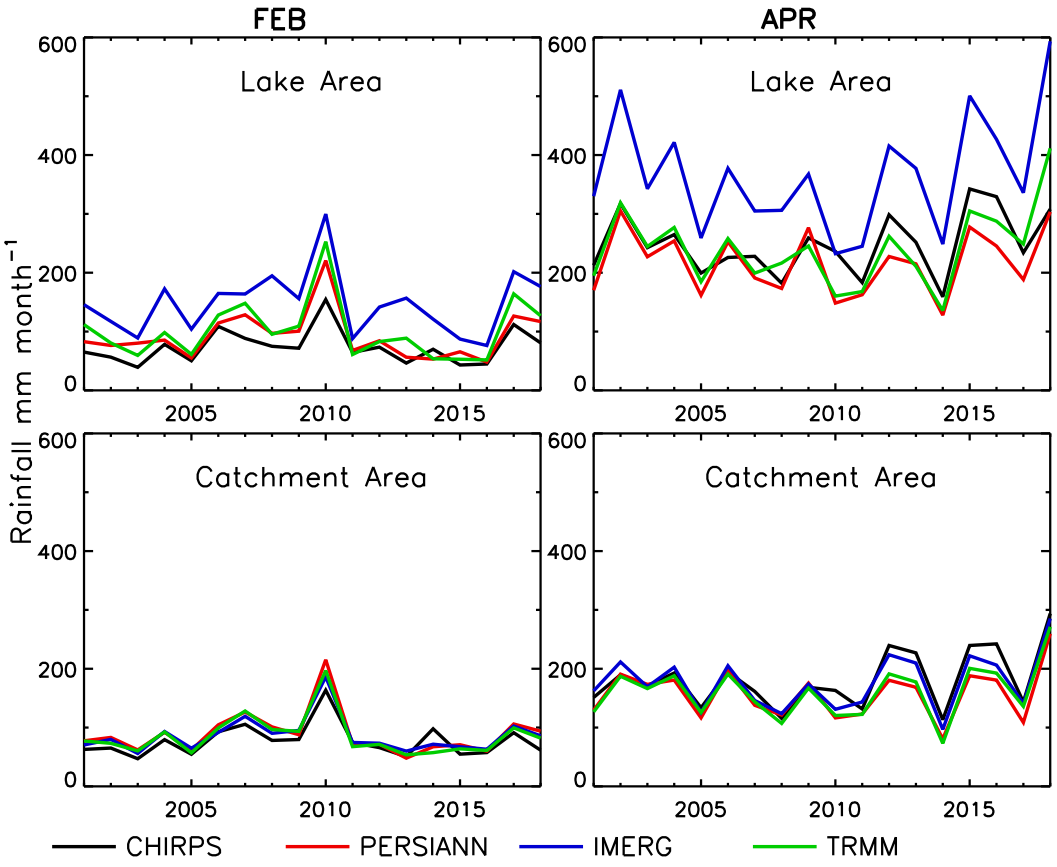

FIG. 5. Interannual variability of rainfall (mm) in April and February from four satellite products.

estimates (828 mm) compared to that for the catchment (112 mm) suggests that some of the satellite products, especially IMERG-F, might have difficulty in assessing the magnitude of overlake rainfall, while capturing the salient features of the spatial pattern of rainfall.

To see if the bias in overlake rainfall is systematic, overlake and catchment rainfall is estimated for two additional eastern African lakes, Tanganyika, and Malawi (Table 1). The work on those lakes will be described in detail in a later publication. As is the case with Lake Victoria, the spread of the estimates is much lower for catchment rainfall than for overlake rainfall. For catchment rainfall the range of estimates is only 46 mm for Lake Malawi and 134 mm for Lake Tanganyika. In contrast, for overlake rainfall the range is 323 mm for Lake Malawi and 474 mm for Lake Tanganyika. For all three lakes, the highest mean for overlake rainfall is with IMERG-F and the lowest means are with CHIRPS2 and PERSIANN-CDR. Although IMERG-F is only a few hundred mm above the other products for Lakes Malawi and Tanganyika, for Lake Victoria it exceeds TRMM 3B43, CHIRPS2, and PERSIANN-CDR by 621, 927, and 828 mm, respectively.

Compared to the other products, IMERG-F clearly overestimates mean rainfall over all three lakes, while showing excellent agreement for catchment rainfall. This suggests a systematic bias in IMERG-F in estimating rainfall over the inland lakes. Further evidence of this is presented in Fig. 5. It depicts monthly averages from 2001 to 2018 for a wet month (April) and a dry month (February). In every case IMERG-F has the highest values of overlake rainfall and in most years it is a clear outlier. In contrast, all four satellite products show extremely close estimates for catchment rainfall in both months in each of the 18 years. This was found to be the case in the remaining months as well (not shown).

Collectively, the results in section 3b suggest the most appropriate product for this study is either CHIRPS2 or TRMM 3B43. Note that for several validations over Africa, TRMM 3B43 was found to outperform PERSIANN (e.g., Beighley et al. 2011; Kizza et al. 2012; Cattani et al. 2016; Nicholson et al. 2019) (see section 2b). The Cattani et al. (2016) study compared the two specifically in the Lake Victoria region. The comparison with overlake rainfall in section 3c also suggests that TRMM 3B43 produces the most reasonable values. Thus the remaining analyses are carried out using TRMM 3B43. The exception is the comparison with MCSs, for which data commence in 1983. To exploit the longer time series, CHIRPS2 is used for that analysis.

4. The seasonal cycle and interannual variability

Lake Victoria lies in the equatorial latitudes where rainfall is concentrated in two seasons (Yang et al. 2015; Nicholson 2017). In the more arid regions of eastern Africa, east of the

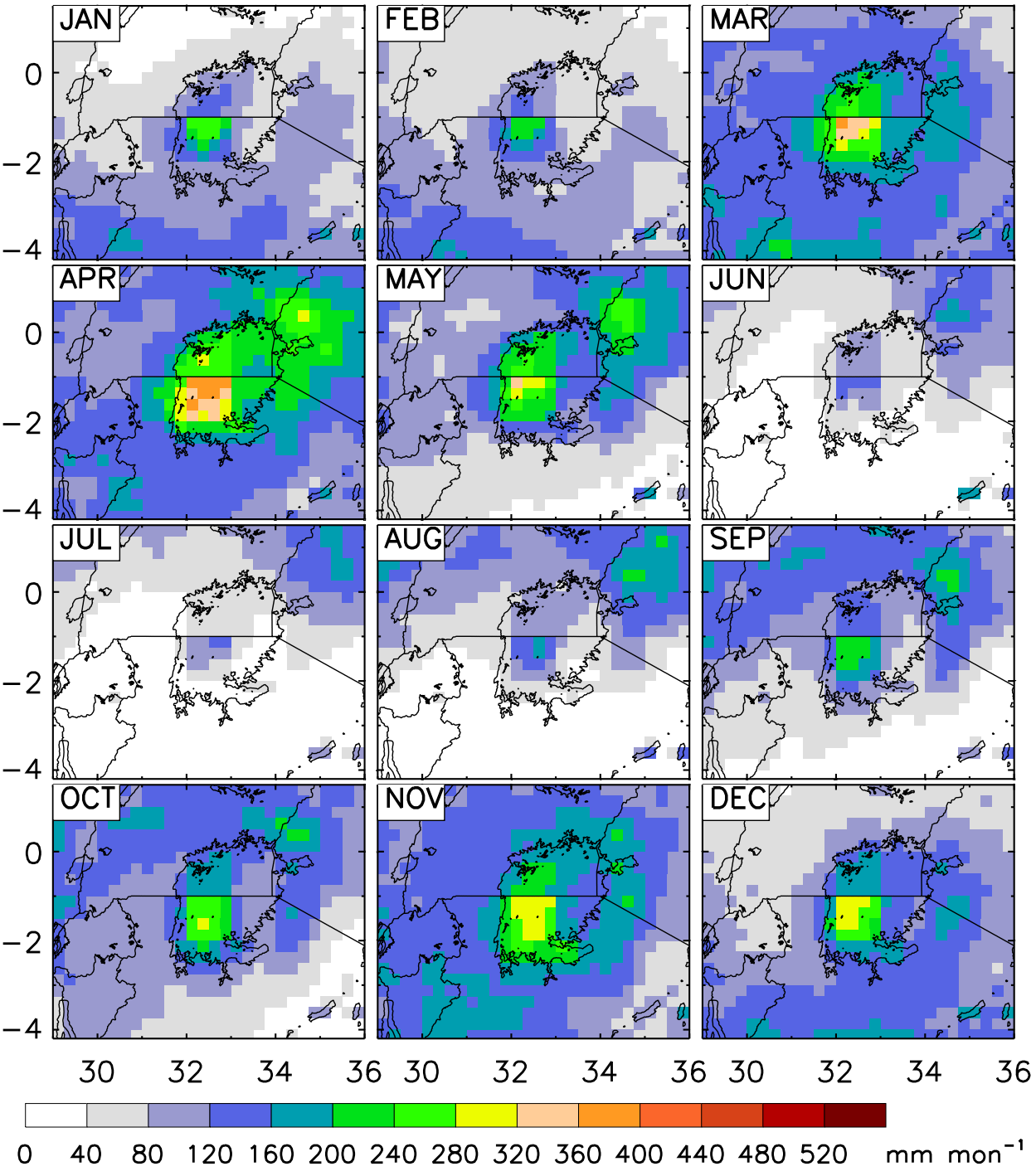

FIG. 6. Maps of monthly rainfall (mm) from TRMM 3B43, averaged for 2001–18.

lake, these are referred to as the "long rains" and the "short rains." The former, the principal rainy season, occur during March–May. The latter occur primarily in October–December. Around the lake and to the west of it the two dry seasons are not intense; mean rainfall exceeds 25 mm in nearly every month.

Traditionally, the two seasons were explained as a consequence of the twice-yearly equatorial transit of the intertropical convergence zone (ITCZ). However, Nicholson (2018) showed that, in fact, this zone does not exist over equatorial Africa. Yang et al. (2015) demonstrated that the rainy seasons are instead associated with increases in surface moist static energy, saturation moist static energy, and vertically integrated moisture flux. Liebmann et al. (2017) concluded that upper-level winds, low-level specific humidity, and convective available potential

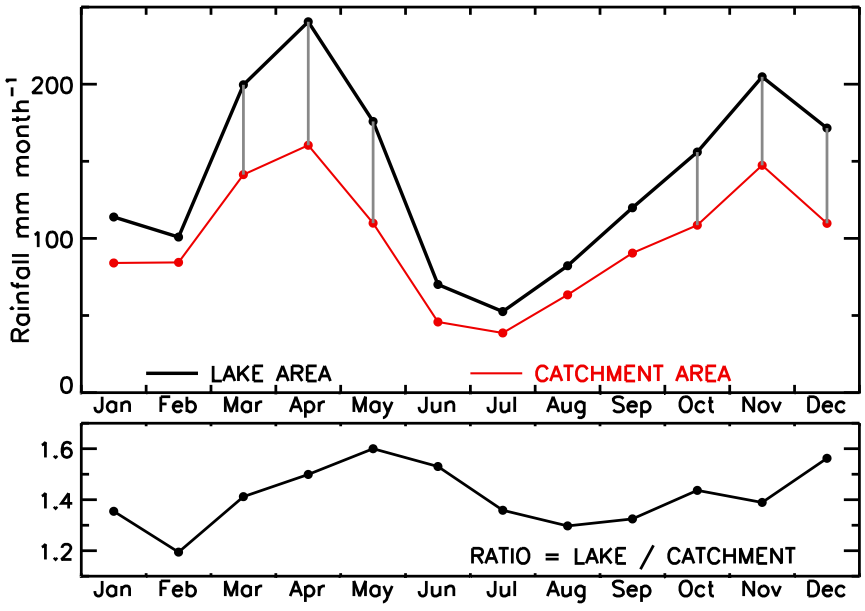

FIG. 7. (top) The seasonal cycle of overlake catchment rainfall and (bottom) the ratio of overlake to catchment rainfall. Vertical dashed lines highlight the contrast during the rainy season months.

energy (CAPE) also play a role. Wind shear might also be a factor (Longandjo 2018).

a. Mean seasonal cycle

Figure 6 shows the seasonal cycle of rainfall over Lake Victoria and its surroundings, based on TRMM 3B43. The driest season over land is from June to September although extensive areas are dry in October in the south and in January and February in the north. An enhancement of rainfall is evident over the lake in every month, even during the dry seasons. The overlake rainfall clearly reaches a maximum during April, but the lake-effect rains are also strong in March, May, October, November, and December. In each month the enhancement is maximized over the western half of the lake. In the southwest quadrant monthly rainfall is on the order of 280 mm or more in March, April, and November.

Figure 7 shows the seasonal cycle averaged over the lake and over its catchment (see Fig. 1). The seasonal cycle is similar in both areas, but the degree of enhancement is strongest during the two rainy seasons, March–May (the long rains) and during October–December (the short rains). The ratio of overlake to catchment rainfall quantifies the enhancement (Fig. 7). It ranges from about 20% in February to over 50% in April through June and in December. It is on the order of 40% during the remaining rainy season months. The greatest enhancement, 60%, is in May.

Thus, the two rainy seasons contrast in two ways (Fig. 7). Both the amount of rainfall and the degree of enhancement over the lake are greater during the March–May season than in the October–December season. However, based on the ratio of overlake to catchment rainfall, the percent enhancement is roughly the same in the two seasons, around 50% during March–May and around 47%–48% during October–December.

The similarity of the seasonal cycle over the lake and over its catchment indicates that the large-scale environment is a major control on rainfall over the lake. The enhancement is well known to be from a combination of lake-land breeze and topographic effects (e.g., Anyah et al. 2006; Thiery et al. 2015). The strength of the easterly trades also has a significant impact (Van de Walle et al. 2020). This will be considered in detail in a later article.

b. Mesoscale convective systems

The presence of MCSs over Lake Victoria is well known. The question examined here is to how these relate to the seasonal cycle and interannual variability of lake-effect rains. Figure 8 shows the total number of MCSs in each half-degree grid box for the months of March–May and for October and November. The MCS dataset does not have information for December. The average is for the years 2001–15, in order to best match the years utilized in Figs. 2 and 3.

In all five months, the MCS count is greatest over western Lake Victoria, and generally within its southwest quadrant. This corresponds to the location of maximum rainfall. The greatest number occur during March and April, when the count exceeds 30 in many of the 0.5° grid boxes. In May, October, and November, when the rainfall maximum in the southwest of the lake is much reduced (Fig. 6), the count is generally on the order of 11–30 in the southwest quadrant of the lake. The MCS count and rainfall are both somewhat higher in November than in the other two months. This suggests that MCS activity is a primary factor in both the amount and spatial distribution of rainfall over the lake. This agrees with Nesbitt et al. (2006),

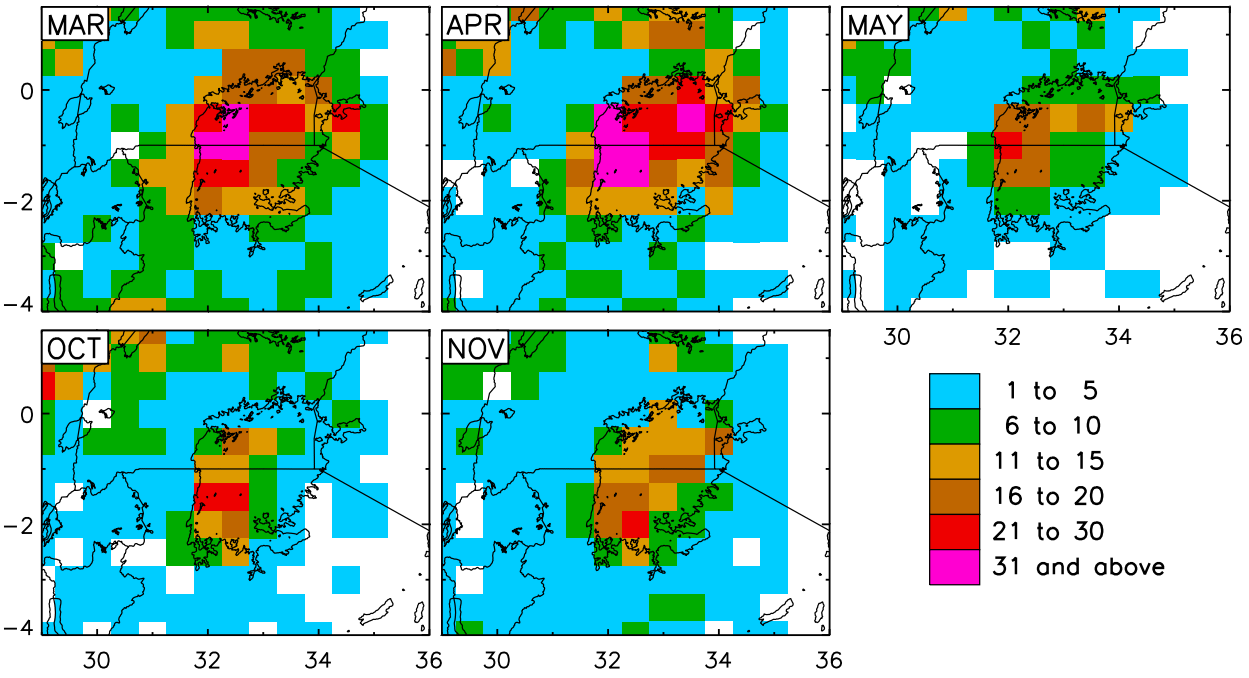

FIG. 8. MCS count by season, totaled within 0.5° blocks. Data are for the years 2001–15.

who found that MCSs account for 50%–60% of the rainfall over Lake Victoria. According to data in Jackson et al. (2009) they account for 75%–85% of the rainfall during the two rainy seasons.

The comparison of MCS count and rainfall over the whole lake area over a period of years further substantiates the link between overlake rainfall and MCS activity. Figure 9 shows rainfall and MCS count for each of the five months from 1983 to 2015. Rainfall is assessed from CHIRPS2 instead of TRMM 3B43, in order to have a longer series of years available. For the five months the correlation between rainfall and MCS count ranges between 0.77 and 0.86, demonstrating a link between the two variables on interannual time scales. The highest correlation is during April, the month of the greatest lake-effect

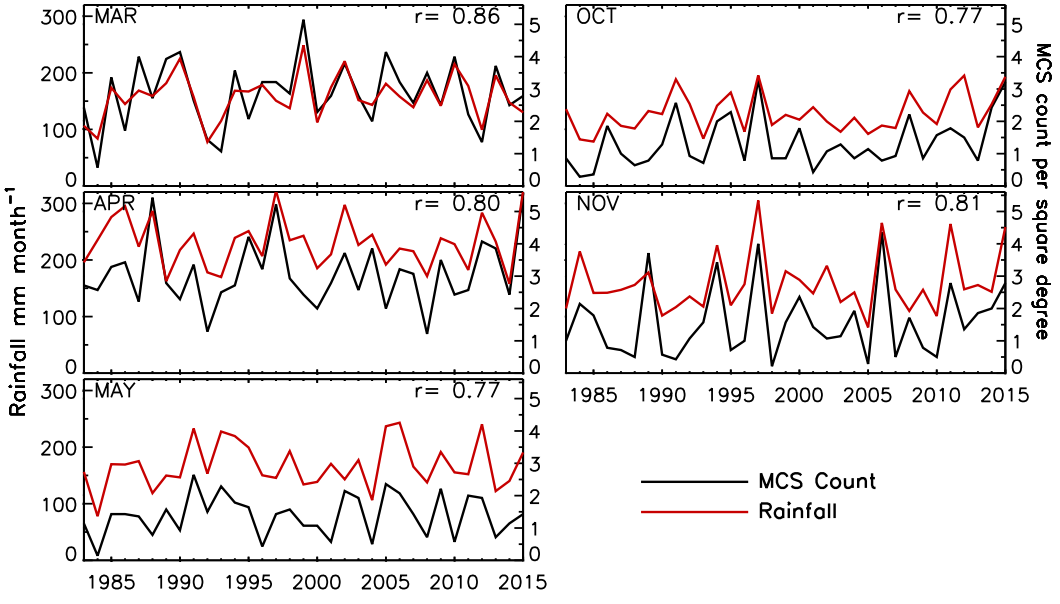

FIG. 9. Number of MCSs vs CHIRPS2 rainfall for each of the five months. Data are averaged for a block enclosing Lake Victoria: 0.5°N–2.5°S, 31.5°–34°E.

TABLE 2. Ratio of average monthly rainfall (mm) to number of mesoscale convective systems during the month.

March	April	May	October	November
55	75	121	97	101

TABLE 3. Mean minimum cloud top temperature (CTT_{min}) and mean maximum area of mesoscale convective systems in each month.

Month	March	April	May	October	November
CTT_{min}	−68	−67	−65	−65	−66
Mean $area_{max}$	4.6	3.8	3.3	3.1	3.5

rains. However, the ratio between the two variables is different in each month (Table 2). It is highest in May, lowest in March, and roughly the same in April and October.

There are two possible interpretations of these figures. One is that higher ratios mean more efficient production of rainfall by individual storms. The other is that higher/lower ratios mean a greater/lower contribution of MCSs to total rainfall. Either way suggests that the contribution of MCS activity to rainfall is different during each month of the rainy seasons. Table 3 shows that average minimum cloud top temperature (CTT) for each month, obtained from GridSat-B1 (Hartman 2020), and the average maximum area of the individual MCSs for each month. CTT indicates that the intensity of the systems is roughly the same in each month. The average maximum area obtained by each system does vary but does not account for the differences in the ratio of rainfall to MCSs. For example, the ratios are very high in May and October, but the maximum areas are the smallest of the five months. This suggests that differences in the ratios represent different contributions of MCSs to total rainfall in five months. If so, MCSs appear to play the greatest role in May and generally a greater role during the short rains than in the long rains season. This is consistent with the percent contribution of convective rainfall determined by Jackson et al. (2009) for the latitudinal sector that includes Lake Victoria: a higher percentage in May than in March and April and higher amounts in October and November than in March and April.

5. Discussion: The overestimation of overlake rainfall by IMERG

IMERG precipitation estimates have been validated via gauge networks over numerous locations globally. The performance is markedly mixed, with relatively good agreement over China (Chen and Li 2016; Wang et al. 2017), the Netherlands (Rios Gaona et al. 2016), and much of Canada (Asong et al. 2017) and poor agreement over Iran (Aslami et al. 2019; Sharifi et al. 2016) and southern Australia (O et al. 2017). In most cases of discrepancies, IMERG overestimates precipitation, tending to overdetect heavy precipitation events (Asong et al. 2017). Over the United States, IMERG overestimated precipitation in the central and eastern United States, but not over the mountainous western regions (Cui et al. 2020; O and Kirstetter 2018). One reason may be that ''morphing'' algorithms may overestimate precipitation because they smooth out the intermittency of convective events (Tian et al. 2009).

IMERG-F clearly has a strong positive and systematic bias over the East African lakes (e.g., Fig. 2 and Table 1). Similarly, Tian and Peters-Lidard (2007) found that TRMM 3B42 and CMORPH exhibited systematic positive rainfall anomalies over inland water bodies in the southeastern United States. Evaluating uncertainties in six TRMM-era satellite-based precipitation estimates globally, Tian and Peters-Lidard (2010) further found that the largest uncertainties are over water bodies. Three of the East African lakes (Victoria, Malawi, and Tanganyika) clearly stand out as areas of high uncertainty, especially during the March–May season, the season of the greatest lake-effect rains. They speculated that the anomalies could be attributed to poor characterization of differences in emissivity and temperature of the water surface in the PMW frequencies used in the retrievals. However, other factors may play a role.

IMERG precipitation retrieval is based on a constellation of PMW sensors (Tan et al. 2019), not all of which are available at a given time and location. Which sensors are available in a given estimate plays a large role in the error of the estimate. Although combined with IR estimates and gauge data, IMERG is primarily influenced by PMW sensors (Guilloteau et al. 2017) and these play a large role in determining IMERG error (Tan et al. 2016). Insufficient PMW sources can also lead to wide discrepancies in the IMERG estimates (O et al. 2017).

The overestimation by IMERG-F of rainfall over Lake Victoria and the other East African lakes is thus most likely associated with PMW retrievals. In particular, this would be associated with the GPROF algorithm, which converts the radiation estimates to rainfall. Overall, the adequacy of IMERG PMW estimates varies with season (Liu 2016), region (e.g., O and Kirstetter 2018), temporal scale (Rios Gaona et al. 2016), and spatial scale (Guilloteau et al. 2017). Several studies have shown that IMERG PMW retrievals tend to overestimate heavy convective precipitation (Asong et al. 2017; O and Kirstetter 2018; Guilloteau et al. 2017). Pre-IMERG PMW retrievals, which utilized an earlier version of the GPROF algorithm (Guilloteau et al. 2017), also tended to overestimate rainfall in convectively active regions and underestimate stratiform precipitation in winter (Tian et al. 2009; Petrović and Kummerow 2017).

O and Kirstetter (2018) showed that IMERG exhibited a significant positive bias in the U.S. Great Plains, where MCSs produce most of the rain and where, like over Lake Victoria, there is a nocturnal rainfall maximum. They suggested that IMERG overestimates the ice components of deep convection at the decaying stage of MCSs, leading to overestimation of both amount and frequency of precipitation.

Guilloteau et al. (2017) examined central and western Africa specifically, finding that IMERG PMW overestimates the amplitude of spatial variations at scales of 20, 40, and 80 km and also the low-pass-filtered variations. This led to an overestimate of spatial variations in precipitation in the Sahel,

which they suggested was a result of systematic overestimation of rain rates for the deep convective systems that are predominant in the Sahel.

The most relevant study for the purpose of our investigation is that of Petković and Kummerow (2017). They evaluated TRMM PMW retrievals, not IMERG, but the results are directly related to the Lake Victoria region. Noting that active microwave estimates are more reliable than passive microwave (Tan et al. 2019; Petković and Kummerow 2017), TRMM PMW was evaluated by comparison with TRMM precipitation radar. They demonstrated that TRMM PMW tends to overestimate precipitation at almost all rainfall rates over central Africa, while underestimating at all rainfall rates over the Amazon. PMW relies on ice scattering to retrieve surface rainfall and this depends strongly on storm dynamics. They concluded that for a given rain rate, ice scattering is enhanced over Africa and depressed over the Amazon, indicating that the cloud microphysical properties are substantially different in the two regions.

The contrast between Central Africa (which includes Lake Victoria) and the Amazon has long been studied and debated, ever since McCollum et al. (2000) noticed that GPCP satellite rainfall estimates over central equatorial Africa were roughly twice as great as the estimates from gauges. Their analysis over the equatorial Amazon showed reasonable GPCP estimates. They hypothesized that the difference may lie in the different microphysical properties of clouds in the two locations. This is consistent with the contrast in storm systems. In Central Africa at least 60%–70% of the rainfall (and possibly as much as 80%) is associated with MCS activity (Nicholson 2021; Jackson et al. 2009), while MCSs contribute little to the rainfall regime over the Amazon (Nesbitt et al. 2000; Zipser et al. 2006).

Notably, most of the rainfall over Lake Victoria is associated with MCSs, as discussed in the section 4b. The analysis of Nesbitt et al. (2006) also suggests that the contribution over Lake Victoria exceeds 50%. The overestimation is consistent with the findings of Asong et al. (2017) and O and Kirstetter (2018), that IMERG PMW retrievals tend to overestimate heavy convective precipitation, and those of Petković and Kummerow (2017), who demonstrated a systematic overestimation of rainfall over Central Africa by the TRMM PMW retrievals. Notably, Tan et al. (2019) demonstrated that IMERG V06 adequately represented the diurnal cycle of precipitation over Lake Victoria. However, an integration of their assessed precipitation rates over the four seasons gave an annual value close to that determined here for IMERG-F, 2338 mm.

Presumably, then, the PMW retrievals of intense convective events are the main reason for overestimation by IMERG of rainfall over Lake Victoria. This of course is related to the GPROF algorithm. However, issues with emissivity and water temperature, as suggested by Tian and Peters-Lidard (2010), cannot be ruled out as additional factors.

It is noteworthy that the estimates from TRMM appear to be realistic, because TRMM retrievals were fused with IMERG to extend the IMERG estimates back to years prior to the GPM launch in 2010. To do this, TRMM data were computed with the GPROF algorithm but different calibrators to produce the extension. Thus, it is necessary to comment on why TRMM 3B43 appears to perform well over Lake Victoria, while IMERG does not. One difference is that TRMM 3B43 is more sensitive to IR retrievals than is IMERG. Notably, CHIRPS2 and PERSIANN-CDR, which are based only on IR estimates, also provide estimates of overlake rainfall that are similar to that of TRMM 3B43 (Fig. 5). TRMM 3B43 and IMERG also use different PMW sensors (Liu 2016) and well as a different GPROF algorithm (Guilloteau et al. 2017).

6. Summary and conclusions

Annual rainfall over Lake Victoria was calculated from four satellite products: TRMM 3B43, CHIRPS2, PERSIANN-CDR, and IMERG-F. The values calculated from these products, respectively, were 1717, 1411, 1510, and 2338 mm. Of these, TRMM 3B43 had the best agreement with long-term means assessed from prior studies, some of which included gauge data over the lake itself. These ranged from 1630 to 1791 mm for periods ranging from 23 to 40 years. Of the prior studies, the most realistic estimate is probably that of Yin and Nicholson (1998), 1791 mm. The value from TRMM 3B43, 1717 mm, is close to that. The value assessed by IMERG-F was clearly an outlier and exceeded the TRMM 3B43 mean by 36%. The rainfall maximum over the lake, as shown in a map published by Flohn and Burkhardt (1985) (Fig. 4) is 3000 mm. TRMM 3B43 indicated some areas with annual rainfall between 3000 and 4000 mm and showed a maximum in the location of that shown on the Flohn–Burkhardt map.

In contrast to the value for overlake rainfall, the values for mean rainfall over the catchment were in close agreement in all four products. The calculated means ranged from 1136 to 1207 mm. A similar result was obtained for Lakes Malawi and Tanganyika: a large overestimation of overlake rainfall by IMERG-F, a large spread of estimates for overlake rainfall, and substantial agreement among the four products for catchment rainfall.

These results suggest IMERG-F has a systematic bias in estimating overlake rainfall, a bias that is confirmed in the analysis of year-to-year rainfall variability in February and April. Past studies of PMW retrievals suggest that the bias of IMERG-F over Lake Victoria is primarily associated with its lower performance in the case of strong precipitation events, such as the MCSs that prevail over Lake Victoria.

For catchment rainfall, gauge data suggest that TRMM 3B43, IMERG-F, and CHIRPS2 provide the best estimates. This is based on an analysis of annual data and data for the month of April. PERSIANN-CDR shows unrealistic values in the high terrain to the east of the lake. For annual rainfall, it shows a large area with rainfall in excess of 1800 mm and a maximum of over 3000 mm. The other satellite and gauge products show rainfall on the order of 1400–1800 mm and only a very small area with rainfall in excess of 1800 mm. The maxima are on the order of 2000–2500 mm. While IMERG-F shows catchment rainfall values similar to those of CHIPRS2 and TRMM 3B43, its failure to adequately assess the magnitude of overlake rainfall precluded it from use in later analyses.

TRMM 3B43 was used to assess the seasonal cycle of rainfall and rainfall enhancement over Lake Victoria. Rainfall was

higher during the long-rains season (March–April) than during the short rains season (October–December). Over both the catchment and the lake, April is the wettest month, with overlake rainfall averaging 240 mm and catchment rainfall averaging roughly 160 mm. The second wettest month is November, with rainfall averaging roughly 205 mm over the lake and 147 mm over the catchment. Rainfall is enhanced over the lake, compared to the catchment, in all months. The ratio of lake to catchment rainfall ranges from a low of 1.2 in February to 1.6 in May. Enhancement is greatest at the end of the two rainy seasons, May and December. In general, it is greater during the long rains than during the short rains.

Despite contrasts in magnitude, the seasonal cycle of overlake rainfall is remarkably similar to that of catchment rainfall. This suggests that the large-scale environment is the major control on rainfall over the lake.

The spatial pattern of MCS activity in each month coincides closely with the spatial pattern of rainfall over the lake and catchment. Maximum MCS activity is over the western to southwestern portion of the lake in all months. As with rainfall, it is greatest in March and April. The interannual variability of rainfall over the lake is highly correlated with the interannual variability of MCS activity in all five months. Overall, the analysis suggests a very large contribution of MCS events to rainfall over Lake Victoria, with the contribution differing in each month. This is consistent with prior estimates of 50%–60% annually (Nesbitt et al. 2006) and 75%–85% during the rainy seasons (Jackson et al. 2009).

This work will continue with an article on the diurnal cycle over Lake Victoria and an article on the lake-effect rains over Lake Tanganyika and Malawi. The current study has shown that TRMM 3B43 will be the most appropriate product for the studies of those lakes.

Acknowledgments. SEN and DK were supported by two grants from the National Science Foundation, GEO/ATM 1854511 and EAR 1850661. The work of ATH was supported by NSF Grant AGS 1535439. We would like to thank an anonymous reviewer for his/her thorough critique of the manuscript and useful suggestions.

Data availability statement. The NIC131 gauge data, the Hartman MCS dataset, and minimum cloud top temperatures can all be obtained by contacting the first author.

REFERENCES

Akurut, M., P. Willems, and C. B. Niwagaba, 2014: Potential impacts of climate change on precipitation over Lake Victoria, East Africa, in the 21st century. *Water*, **6**, 2634–2659, https://doi.org/10.3390/w6092634.

Anyah, R. O., F. H. M. Semazzi, and L. Xie, 2006: Simulated physical mechanisms associated with climate variability over Lake Victoria basin in East Africa. *Mon. Wea. Rev.*, **134**, 3588–3609, https://doi.org/10.1175/MWR3266.1.

Ashouri, H., K. L. Hsu, S. Sorooshian, D. K. Braithwaite, K. R. Knapp, L. D. Cecil, B. R. Nelson, and O. P. Prat, 2015: PERSIANN- CDR: Daily precipitation climate data record from multisatellite observations for hydrological and climate studies. *Bull. Amer. Meteor. Soc.*, **96**, 69–83, https://doi.org/10.1175/BAMS-D-13-00068.1.

Aslami, F., A. Ghorbani, B. Sobhani, and A. Esmali, 2019: Comprehensive comparison of daily IMERG and GSMaP satellite precipitation products in Ardabil Province, Iran. *Int. J. Remote Sens.*, **40**, 3139–3153, https://doi.org/10.1080/01431161.2018.1539274.

Asong, Z. E., S. Razavi, H. S. Wheater, and J. S. Wong, 2017: Evaluation of Integrated Multisatellite Retrievals for GPM (IMERG) over southern Canada against ground precipitation observations: A preliminary assessment. *J. Hydrometeor.*, **18**, 1033–1050, https://doi.org/10.1175/JHM-D-16-0187.1.

Awange, J. L., V. G. Ferreira, E. Forootan, S. A. Khandu, S. A. Andam-Akorful, N. O. Agutu, and X. F. He, 2016: Uncertainties in remotely sensed precipitation data over Africa. *Int. J. Climatol.*, **36**, 303–323, https://doi.org/10.1002/joc.4346.

Ba, M. B., and S. E. Nicholson, 1998: Analysis of convective activity and its relationship to the rainfall over the Rift Valley lakes of East Africa during 1983-90 using Meteosat infrared channel. *J. Appl. Meteor.*, **37**, 1250–1264, https://doi.org/10.1175/1520-0450(1998)037<1250:AOCAAI>2.0.CO;2.

Beighley, R. E., and Coauthors, 2011: Comparing satellite derived precipitation datasets using the Hillslope River Routing (HRR) model in the Congo River basin. *Hydrol. Processes*, **25**, 3216–3229, https://doi.org/10.1002/hyp.8045.

Bergonzini, L., 1998: Bilans hydriques de lacs (Kivu, Tanganyika, Rukwa et Nyassa) du rift Est-Africain. Musée Royal de l'Afrique Centrale de Tervuren Belgique Annales des Sciences Géologiques, Vol. 103, Musée Royal de l'Afrique Centrale, 183 pp.

——, Y. Richard, and P. Camberlin, 2002: Interannual variation of the water budget of Lake Tanganyika (1932-1995): Changes in the precipitation-lake water excess relationship. *Hydrol. Sci. J.*, **47**, 781–796, https://doi.org/10.1080/02626660209492980.

Camberlin, P., and Coauthors, 2019: Evaluation of remotely sensed rainfall products over central Africa. *Quart. J. Roy. Meteor. Soc.*, **145**, 2115–2138, https://doi.org/10.1002/qj.3547.

Cattani, E., A. Merino, and V. Levizzani, 2016: Evaluation of monthly satellite-derived precipitation products over East Africa. *J. Hydrometeor.*, **17**, 2555–2573, https://doi.org/10.1175/JHM-D-15-0042.1.

Chebud, Y. A., and A. M. Melesse, 2009: Modelling lake stage and water balance of Lake Tana, Ethiopia. *Hydrol. Processes*, **23**, 3534–3544, https://doi.org/10.1002/hyp.7416.

Chen, F., and X. Li, 2016: Evaluation of IMERG and TRMM 3B43 monthly precipitation products over Mainland China. *Remote Sens.*, **8**, 472, https://doi.org/10.3390/rs8060472.

Cui, W., X. Dong, B. Xi, Z. Feng, and J. W. Fan, 2020: Can the GPM IMERG Final Product accurately represent MCSs precipitation characteristics over the central and eastern United States? *J. Hydrometeor.*, **21**, 39–57, https://doi.org/10.1175/JHM-D-19-0123.1.

Datta, R. K., 1981: Certain aspects of monsoonal precipitation dynamics over Lake Victoria. *Monsoon Dynamics*, J. Lighthill and R. Pearce, Eds., Cambridge Press, 333–348.

Dezfuli, A. K., C. M. Ichoku, G. J. Huffman, K. I. Mohr, J. S. Selker, N. van de Giesen, R. Hochreutener, and F. O. Annor, 2017: Validation of IMERG precipitation in Africa. *J. Hydrometeor.*, **18**, 2817–2825, https://doi.org/10.1175/JHM-D-17-0139.1.

Di Baldassarre, G., and Coauthors, 2011: Future hydrology and climate in the River Nile basin: A review. *Hydrol. Sci. J.*, **56**, 199–211, https://doi.org/10.1080/02626667.2011.557378.

Dinku, T., C. Funk, P. Peterson, R. Maidment, T. Tadesse, H. Gadain, and P. Ceccato, 2018: Validation of the CHIRPS

satellite rainfall estimates over eastern Africa. *Quart. J. Roy. Meteor. Soc.*, **144**, 292–312, https://doi.org/10.1002/qj.3244.

Flohn, H., 1983: Das Katastrophenregen 1961/62 und die Wasserbilanz des Viktoria-See-Gebietes. *Wiss. Ber. Meteor. Inst. Univ. Karlsruhe*, **4**, 17–34.

——, and K. Fraedrich, 1966: Tagesperiodische Zirkulation und Niederschlagsverteilung am Victoria-See (Ostafrika). *Meteor. Rundsch.*, **19**, 157–165.

——, and T. Burkhardt, 1985: Nile runoff at Aswan and Lake Victoria; an example of a discontinuous climate time series. *Z. Gletschkd. Glazialgeol.*, **21**, 125–130.

Fraedrich, K., 1968: Das Land- und Seewindsystem des Victoria-Sees nach aerologischen Daten. *Arch. Meteor. Biokl. Geophys.*, **17A**, 186–206.

——, 1971: Modell einer lokalen atmosphärischen Zirkulation mit Anwendung auf den Victoria-See. *Beitr. Phys. Atmos.*, **44**, 95–114.

——, 1972: A simple climatological model of the dynamics and energetics of the nocturnal circulation at Lake Victoria. *Quart. J. Roy. Meteor. Soc.*, **98**, 322–335, https://doi.org/10.1002/qj.49709841606.

Funk, C. C., S. E. Nicholson, M. Landsfeld, D. A. Klotter, P. Peterson, and L. Harrison, 2015: The Centennial Trends Greater Horn of Africa precipitation dataset. *Sci. Data*, **2**, 150050, https://doi.org/10.1038/sdata.2015.50.

Guilloteau, C., E. Foufoula-Georgiou, and C. D. Kummerow, 2017: Global multiscale evaluation of satellite passive microwave retrieval of precipitation during TRMM and GPM eras: Effective resolution and regional diagnostics for future algorithm development. *J. Hydrometeor.*, **18**, 3051–3070, https://doi.org/10.1175/JHM-D-17-0087.1.

Haile, A. T., E. Habib, M. Elsaadani, and T. Rientjes, 2013: Inter-comparison of satellite rainfall products for representing rainfall diurnal cycle over the Nile basin. *Int. J. Appl. Earth Obs. Geoinf.*, **21**, 230–240, https://doi.org/10.1016/j.jag.2012.08.012.

Hartman, A. T., 2016: Tracking and analysis of mesoscale convective systems over central equatorial Africa. M.S. thesis, Dept. of Earth, Ocean, and Atmospheric Science, Florida State University, 68 pp., http://purl.flvc.org/fsu/fd/FSU_FA2016_Hartman_fsu_0071N_13642.

——, 2020: Tracking mesoscale convective systems in central equatorial Africa. *Int. J. Climatol.*, **41**, 469–482, https://doi.org/10.1002/joc.6632.

Howell, P., M. Lock, and S. Cobb, 1988: *The Jonglei Canal: Impact and Opportunity*. Cambridge University Press, 537 pp.

Huffman, G. J., and D. T. Bolvin, 2014: TRMM and other data precipitation data set documentation. NASA TRMM Doc., 42 pp., ftp://precip.gsfc.nasa.gov/pub/trmmdocs/3B42_3B43_doc.pdf.

——, and Coauthors, 2007: The TRMM Multisatellite Precipitation Analysis: Quasi-global, multi-year, combined-sensor precipitation estimates at finer scale. *J. Hydrometeor.*, **8**, 38–55, https://doi.org/10.1175/JHM560.1.

——, D. T. Bolvin, and E. J. Nelkin, 2015: Day 1 IMERG Final Run release notes. NASA Doc., 9 pp., http://pmm.nasa.gov/sites/default/files/document_files/IMERG_FinalRun_Day1_release_notes.pdf.

——, ——, ——, and J. Tan, 2019: Integrated Multi-satellitE Retrievals for GPM (IMERG) technical documentation. NASA Tech. Doc., 71 pp., https://pmm.nasa.gov/data-access/downloads/gpm.

Jackson, B., S. E. Nicholson, and D. Klotter, 2009: Mesoscale convective systems over western equatorial Africa and their relationship to large-scale circulation. *Mon. Wea. Rev.*, **137**, 1272–1294, https://doi.org/10.1175/2008MWR2525.1.

Kebede, S., Y. Travi, T. Alemayehu, and V. Marc, 2006: Water balance of Lake Tana and its sensitivity to fluctuations in rainfall, Blue Nile basin, Ethiopia. *J. Hydrol.*, **316**, 233–247, https://doi.org/10.1016/j.jhydrol.2005.05.011.

Kizza, M., I. Westerberg, A. Rodhe, and H. K. Ntale, 2012: Estimating areal rainfall over Lake Victoria and its basin using ground-based and satellite data. *J. Hydrol.*, **464–465**, 401–411, https://doi.org/10.1016/j.jhydrol.2012.07.024.

Lehman, J., 2002: Application of AVHRR to water balance, mixing dynamics, and water chemistry of Lake Edward, East Africa. *The East African Great Lakes: Limnology, Palaeolimnology, Biodiversity*, E. O. Odada and D. Olago, Eds., Springer Science & Business Media, 235–260.

Liebmann, B., and Coauthors, 2017: Climatology and interannual variability of boreal spring wet season precipitation in the eastern Horn of Africa and implications for its recent decline. *J. Climate*, **30**, 3867–3886, https://doi.org/10.1175/JCLI-D-16-0452.1.

Liu, Z., 2016: Comparison of Integrated Multisatellite Retrievals for GPM (IMERG) and TRMM Multisatellite Precipitation Analysis (TMPA) monthly precipitation products: Initial results. *J. Hydrometeor.*, **17**, 777–790, https://doi.org/10.1175/JHM-D-15-0068.1.

Longandjo, G.-N. T., 2018: The hydroclimate variability of Central Africa: Seasonal cycle, mechanisms, teleconnections and impacts on neighbouring regions. Ph.D. thesis, University of Cape Town, 165 pp.

Lyons, R. P., C. N. Kroll, and C. A. Scholz, 2011: An energy balance hydrologic model for the Lake Malawi Rift Basin, East Africa. *Global Planet. Change*, **75**, 83–97, https://doi.org/10.1016/j.gloplacha.2010.10.010.

McCollum, J. R., A. Gruber, and M. B. Ba, 2000: Discrepancy between gauges and satellite estimates of rainfall in equatorial Africa. *J. Appl. Meteor.*, **39**, 666–679, https://doi.org/10.1175/1520-0450-39.5.666.

Munzimi, Y., M. Hansen, B. Adusei, and G. Senay, 2015: Characterizing Congo Basin rainfall and climate using Tropical Rainfall Measuring Mission (TRMM) satellite data and limited rain gauge ground observations. *J. Appl. Meteor. Climatol.*, **54**, 541–556, https://doi.org/10.1175/JAMC-D-14-0052.1.

Muvundja, F. A., A. Wüest, M. Isumbisho, M. B. Kaningini, N. Pasche, P. Rinta, and M. Schmid, 2014: Modelling Lake Kivu water level variations over the last seven decades. *Limnologica*, **47**, 21–33, https://doi.org/10.1016/j.limno.2014.02.003.

Nesbitt, S. W., E. J. Zipser, and D. J. Cecil, 2000: A census of precipitation features in the tropics using TRMM: Radar, ice scattering, and ice observations. *J. Climate*, **13**, 4087–4106, https://doi.org/10.1175/1520-0442(2000)013<4087:ACOPFI>2.0.CO;2.

——, R. Cifelli, and S. A. Rutledge, 2006: Storm morphology and rainfall characteristics of TRMM precipitation features. *Mon. Wea. Rev.*, **134**, 2702–2721, https://doi.org/10.1175/MWR3200.1.

Nicholson, S. E., 2017: Climate and climatic variability of rainfall over eastern Africa. *Rev. Geophys.*, **55**, 590–635, https://doi.org/10.1002/2016RG000544.

——, 2018: The ITCZ and the seasonal cycle over equatorial Africa. *Bull. Amer. Meteor. Soc.*, **99**, 337–348, https://doi.org/10.1175/BAMS-D-16-0287.1.

——, 2021: The rainfall and convective regime over equatorial Africa, with emphasis on the Congo Basin. *Congo Basin*

Hydrology, Climate, and Biogeochemistry: A Foundation for the Future, D. Alsdorf, R. Tshimanga, and G. Moukandi, Eds., Amer. Geophys. Union, in press.

——, and X. G. Yin, 2002: Mesoscale patterns of rainfall, cloudiness and evaporation over the Great Lakes of East Africa. *The East African Great Lakes: Limnology, Palaeolimnology and Biodiversity*, E. O. Odada and D. Olago, Eds., Springer Science & Business Media, 93–119.

——, C. Funk, and A. Fink, 2018: Rainfall over the African continent from the 19th through 21st century. *Global Planet. Change*, **165**, 114–127, https://doi.org/10.1016/j.gloplacha.2017.12.014.

——, D. Klotter, L. Zhou, and W. Hua, 2019: Validation of satellite precipitation estimates over the Congo Basin. *J. Hydrometeor.*, **20**, 631–656, https://doi.org/10.1175/JHM-D-18-0118.1.

O, S., and P.-E. Kirstetter, 2018: Evaluation of diurnal variation of GPM IMERG-derived summer precipitation over the contiguous US using MRMS data. *Quart. J. Roy. Meteor. Soc.*, **144**, 270–281, https://doi.org/10.1002/qj.3218.

——, U. Foelsche, G. Kirchengast, J. Fuchsberger, J. Tan, and W. A. Petersen, 2017: Evaluation of GPM IMERG early, late, and final rainfall estimates using WegenerNet gauge data in southeastern Austria. *Hydrol. Earth Syst. Sci.*, **21**, 6559–6572, https://doi.org/10.5194/hess-21-6559-2017.

Ogallo, L. J., P. Bessemoulin, J. P. Ceron, S. Mason, and S. J. Connor, 2008: Adapting to climate variability and change: The climate outlook forum process. *WMO Bull.*, **57**, 93–102.

Petković, V., and C. D. Kummerow, 2017: Understanding the sources of satellite passive microwave rainfall retrieval systematic errors over land. *J. Appl. Meteor. Climatol.*, **56**, 597–614, https://doi.org/10.1175/JAMC-D-16-0174.1.

Rientjes, T. H. M., B. U. J. Perera, A. T. Haile, P. Reggiani, and L. P. Muthuwatta, 2011: Regionalisation for lake level simulation - The case of Lake Tana in the Upper Blue Nile, Ethiopia. *Hydrol. Earth Syst. Sci.*, **15**, 1167–1183, https://doi.org/10.5194/hess-15-1167-2011.

Rios Gaona, M. F., A. Overeem, H. Leijnse, and R. Uijlemhoet, 2016: First-year evaluation of GPM rainfall over the Netherlands: IMERG Day 1 Final Run (V03D). *J. Hydrometeor.*, **17**, 2799–2814, https://doi.org/10.1175/JHM-D-16-0087.1.

Sene, K. J., 2000: Theoretical estimates for the influence of Lake Victoria on flows in the upper White Nile. *Hydrol. Sci. J.*, **45**, 125–145, https://doi.org/10.1080/02626660009492310.

Sharifi, E., R. Steinacker, and B. Saghafian, 2016: Assessment of GPM-IMERG and other precipitation products against gauge data under different topographic and climatic conditions in Iran: Preliminary results. *Remote Sens.*, **8**, 135, https://doi.org/10.3390/rs8020135.

Swenson, S., and J. Wahr, 2009: Monitoring the water balance of Lake Victoria, East Africa, from space. *J. Hydrol.*, **370**, 163–176, https://doi.org/10.1016/j.jhydrol.2009.03.008.

Tan, J., W. A. Petersen, and A. Tokay, 2016: A novel approach to identify sources of errors in IMERG for GPM ground validation. *J. Hydrometeor.*, **17**, 2477–2491, https://doi.org/10.1175/JHM-D-16-0079.1.

——, G. J. Huffman, D. T. Bolvin, and E. J. Nelkin, 2019: Diurnal cycle of IMERG V06 precipitation. *Geophys. Res. Lett.*, **46**, 13 584–13 592, https://doi.org/10.1029/2019GL085395.

Tate, E., J. Sutcliffe, D. Conway, and F. Farquharson, 2004: Water balance of Lake Victoria: Update to 2000 and climate change modelling to 2100. *Hydrol. Sci. J.*, **49**, 563–574, https://doi.org/10.1623/hysj.49.4.563.54422.

Thiery, W., E. L. Davin, H. J. Panitz, M. Demuere, S. Lhermitte, and N. van Lipzig, 2015: The impact of the African Great Lakes on regional climate. *J. Climate*, **28**, 4061–4085, https://doi.org/10.1175/JCLI-D-14-00565.1.

Tian, Y., and C. D. Peters-Lidard, 2007: Systematic anomalies over inland water bodies in satellite-based precipitation estimates. *Geophys. Res. Lett.*, **34**, L14403, https://doi.org/10.1029/2007GL030787.

——, and ——, 2010: A global map of uncertainties in satellite-based precipitation measurements. *Geophys. Res. Lett.*, **37**, L24407, https://doi.org/10.1029/2010GL046008.

——, and Coauthors, 2009: Component analysis of errors in satellite-based precipitation estimates. *J. Geophys. Res.*, **14**, D24101, https://doi.org/10.1029/2009JD011949.

Tigabu, T. B., P. D. Wagner, G. Hoermann, and N. Fohrer, 2019: Modeling the impact of agricultural crops on the spatial and seasonal variability of water balance components in the Lake Tana basin, Ethiopia. *Hydrol. Res.*, **50**, 1376–1396, https://doi.org/10.2166/nh.2019.170.

Vanderkelen, I., N. P. N. van Lipzig, and W. Thiery, 2018: Modelling the water balance of lake Victoria (East Africa) - Part 1: Observational analysis. *Hydrol. Earth Syst. Sci.*, **22**, 5509–5525, https://doi.org/10.5194/hess-22-5509-2018.

Van de Walle, J., W. Thiery, O. Brousse, N. Souverijns, M. Demuzere, and N. P. M. van Lipzig, 2020: A convection-permitting model for the Lake Victoria Basin: Evaluation and insight into the mesoscale versus synoptic atmospheric dynamics. *Climate Dyn.*, **54**, 1779–1799, https://doi.org/10.1007/s00382-019-05088-2.

Velpuri, N. M., G. B. Senay, and K. O. Asante, 2012: A multi-source satellite data approach for modelling Lake Turkana water level: Calibration and validation using satellite altimetry data. *Hydrol. Earth Syst. Sci.*, **16**, 1–18, https://doi.org/10.5194/hess-16-1-2012.

Wale, A., T. H. M. Rientjes, A. S. M. Gieske, and H. A. Getachew, 2009: Ungauged catchment contributions to Lake Tana's water balance. *Hydrol. Processes*, **23**, 3682–3693, https://doi.org/10.1002/hyp.7284.

Wang, Z. L., R. D. Zhong, C. G. Lai, and J. C. Chen, 2017: Evaluation of the GPM IMERG satellite-based precipitation products and the hydrological utility. *Atmos. Res.*, **196**, 151–163, https://doi.org/10.1016/j.atmosres.2017.06.020.

Yang, W., R. Seager, M. A. Cane, and B. Lyon, 2015: The annual cycle of East African precipitation. *J. Climate*, **28**, 2385–2404, https://doi.org/10.1175/JCLI-D-14-00484.1.

Yin, X. G., and S. E. Nicholson, 1998: The water balance of Lake Victoria. *Hydrol. Sci. J.*, **43**, 789–811, https://doi.org/10.1080/02626669809492173.

——, and ——, 2002: Interpreting annual rainfall from the levels of Lake Victoria. *J. Hydrometeor.*, **3**, 406–416, https://doi.org/10.1175/1525-7541(2002)003<0406:IARFTL>2.0.CO;2.

Zipser, E. J., D. J. Cecil, C. Liu, S. W. Nesbitt, and D. P. Yorty, 2006: Where are the most intense thunderstorms on earth? *Bull. Amer. Meteor. Soc.*, **87**, 1057–1072, https://doi.org/10.1175/BAMS-87-8-1057.